Enhanced Visible-Light-Driven Photocatalytic performances using Bi_2WO_6/ MS (M= Cd, Zn) heterostructures: Facile synthesis and their photocatalytic mechanisms

Rongfeng Tang, Huaifen Su, Shengxia Duan, Yuanwei Sun, Lei Li, Xianxi Zhang, Suyuan Zeng * and Dezhi Sun *

Shandong Provincial Key Laboratory of Chemical Energy Storage and Novel Cell Technology, Department of Chemistry and Chemical Engineering, Liaocheng University, Liaocheng 252059, China

Corresponding author: Suyuan Zeng and Dezhi Sun. Tel: +86-635-8230614, Fax: +86-635-8230196. Email: drzengsy@163.com, sundezhi@lcu.edu.cn

Appendix A. Supplementary material

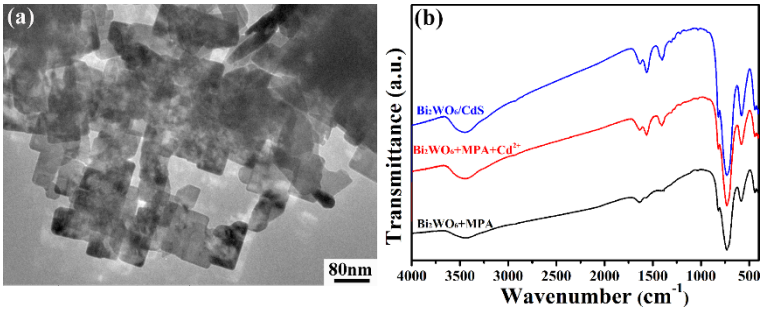

Fig. S1. (a) TEM imagines of sample Bi_2WO_6/CdS; (b) FTIR spectra of sample Bi_2WO_6/CdS, Bi_2WO_6+MPA+Cd^{2+}, and Bi_2WO_6+MPA.

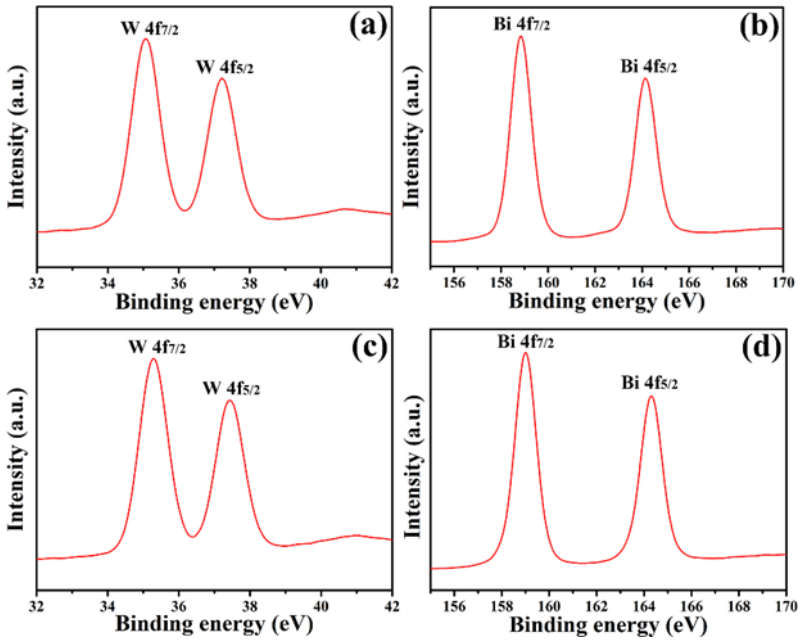

Fig. S2. XPS analysis of (a) W 4f and (b) Bi 4f of Bi_2WO_6/CdS sample; (c) W 4f and (d) Bi 4f of Bi_2WO_6/ZnS sample.

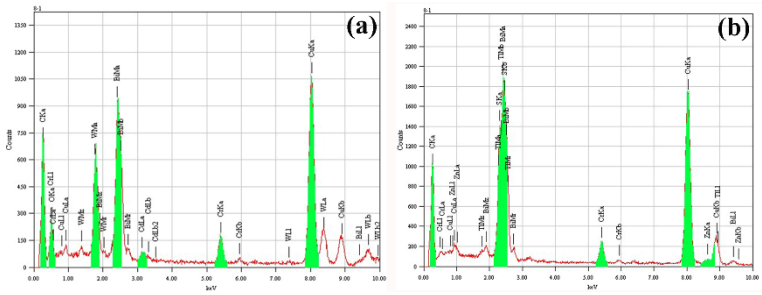

Fig. S3. EDS spectra of the composite photocatalysts: (a) Bi_2WO_6/CdS, (b) Bi_2WO_6/ZnS.

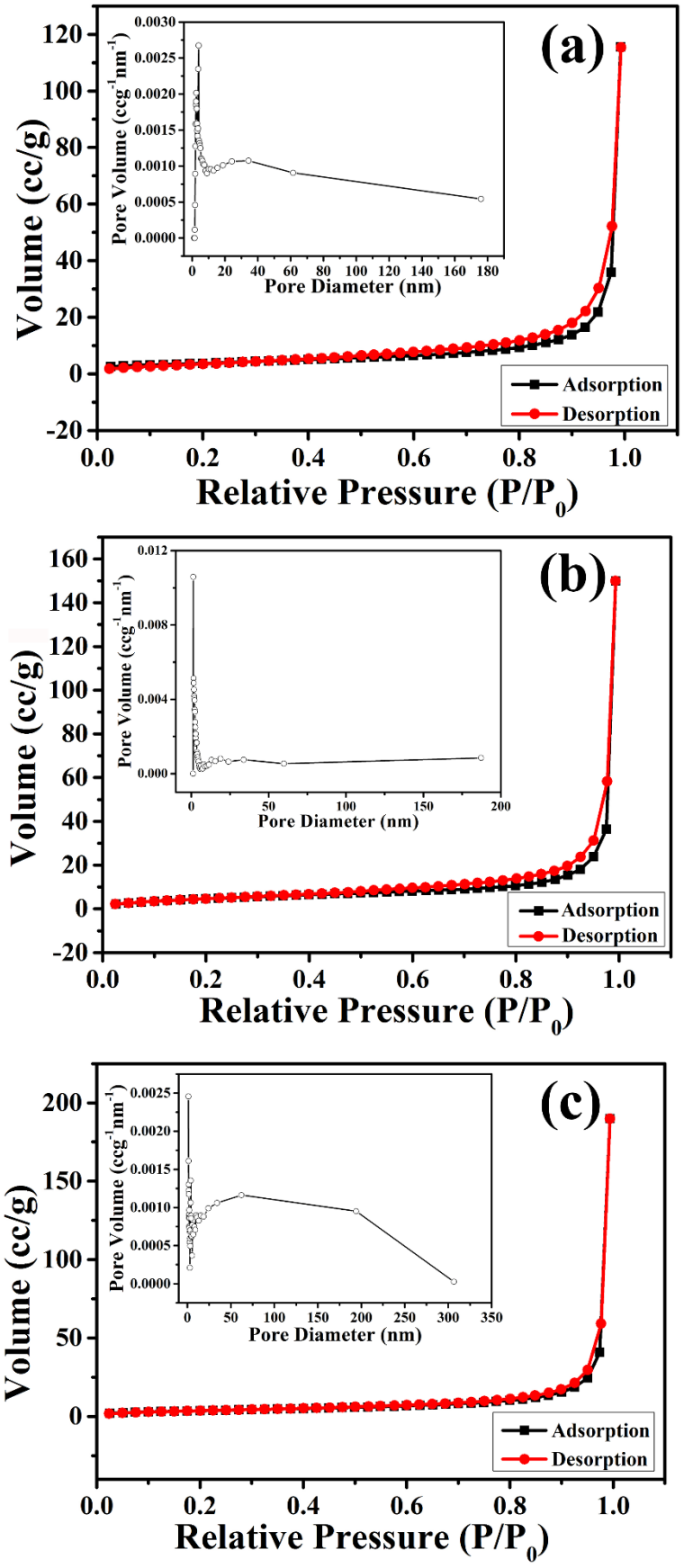

Fig. S4. Nitrogen adsorption−desorption isotherms and the pore size distribution curve

(inset) of samples (a) BW, (b) BW-Cd, and (c) BW-Zn.

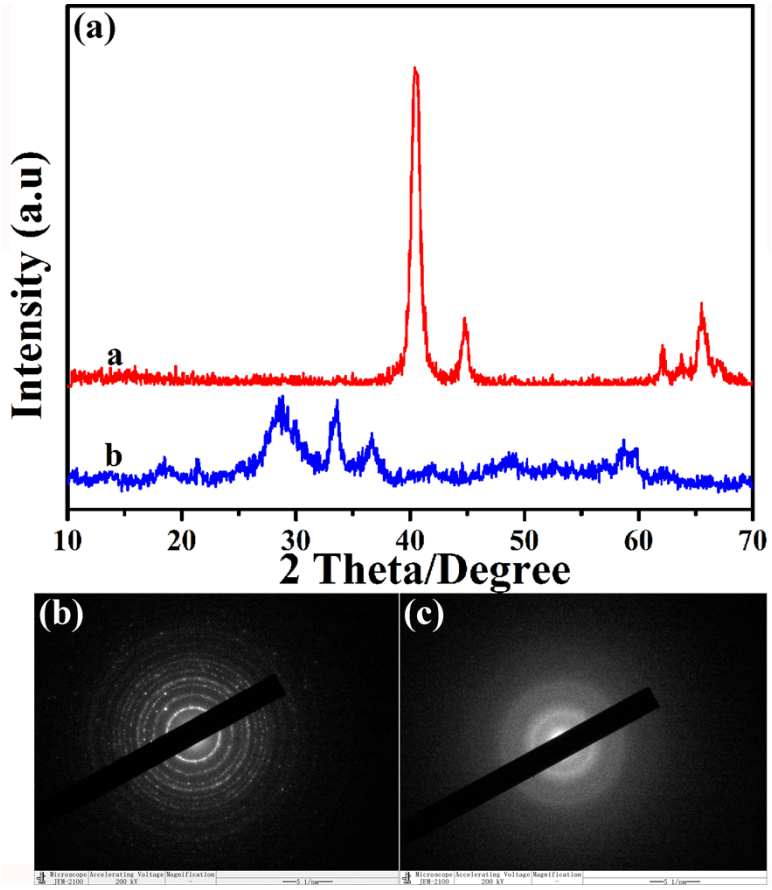

Fig. S5. XRD patterns of sample (a) P25 and Bi_2WO_6, (b-c) SAED patterns of P25 and ZnS nanoparticles.

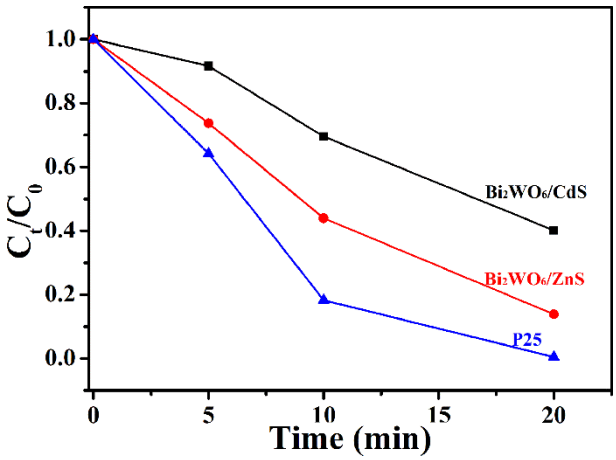

Fig. S6. Photocatalytic performance of sample P25, Bi_2WO_6/CdS and Bi_2WO_6/ZnS under UV-light.

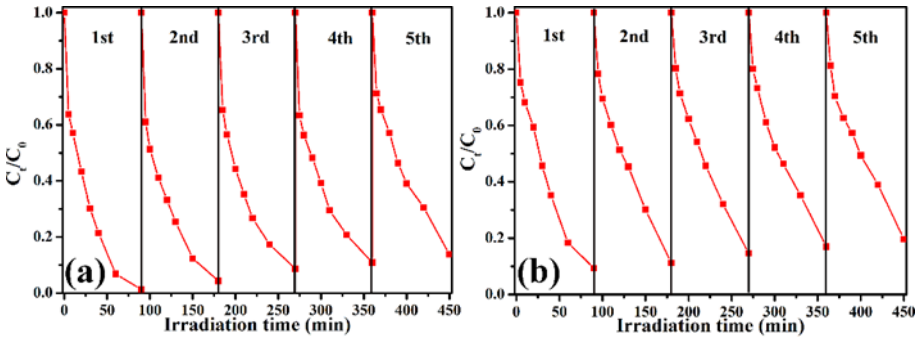

Fig. S7. Cycling runs of the photocatalytic degradation for RhB in the presence of (a) BW-Cd, and (b) BW-Zn under visible light.

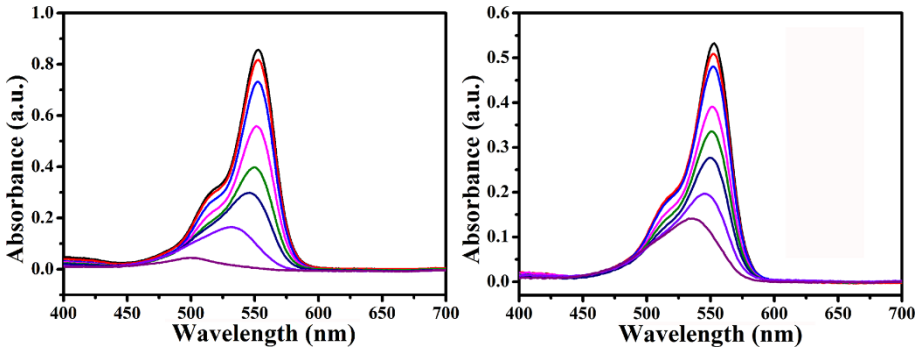

Fig. S8. The temporal evolution of RhB absorption spectra over (a) BW-Cd and (b) BW-Zn.